Feasibility of a Virtual Constellation using Small Aperture, Wide Field of View Optical Systems for Space Domain Awareness and Applications

Siddharth Dave
York University
Regina S. K. Lee
York University

ABSTRACT

The paper outlines a virtual constellation concept of cameras on satellites that have potential to provide near real-time information of other satellites that are detected in orbit. The work presented discusses constellation population and spread, image processing algorithms and computational hardware, optics and imager, space domain awareness contributing sensor and accuracy requirements. The research evaluates the pros and cons of the described approach to space domain awareness and outlines why it can be a valuable contribution to current space surveillance needs. The paper also outlines future applications that can emerge from building such a large database using machine learning and artificial intelligence.

1. INTRODUCTION

Earth orbit is more congested and congestion leads to an increase in the probability of collision between two orbiting objects. Just like how we value environmental protection on Earth, future of the Earth-centric space industry must be conducted safely and sustainably. Space domain awareness (SDA) and space traffic management (STM) are near real-time continuous operations that require constant effort, in part due to the chaotic weather-like nature of orbiting bodies. Factors such as solar radiation pressure, resident space object (RSO) attitude, orbital maneuvers, atmospheric density fluctuation and outgassing drastically alter from propagation models. Fundamentally, the only way to have a precise, real-time, and holistic awareness of all objects in Earth orbit is by establishing a network to continuously monitor it. Automation is key for such a surveillance network. The Space Surveillance Network (SSN) provides a majority of the data used for SDA. The SSN detects, tracks, identifies and maintains a catalog of over 26,000 objects in Earth orbit [1]. The publicly available catalog at *space-track.org* is a part of the United States Space Command's (USSPACECOM) commitment to information sharing to promote a safe and sustainable space environment.

In its current state, our SDA does not meet the desired objectives [2] [1], especially for low Earth orbit (LEO). The key limitations of the SSN for LEO, as summarized by April [3], are instrument count, geographical distribution, capability and availability. Instruments currently used for surveillance are expensive to build, maintain, and replace. Due to their high cost, fewer are built. Ground-based telescopes are limited by geographical location, weather, daylight hours and tracking constraints. Ground-based tracking radar is ideal for range and velocity measurements of RSO up to 1 cm in diameter. However, radar is limited by geographical location, transmission power, and resolution of RSO characterization. Missions like Space-Based Visible (SBV) [4] [5], Sapphire [6], and NEOSSat [7] have successfully demonstrated how space-based instruments can contribute to our awareness, and the progressive capabilities of technology demonstrated highlight the need for further missions. However, the concept of operations (CONOPS) for the space-based SDA missions do not solve the limitations of geographical distribution and instrument count, and hence struggle with LEO-LEO surveillance. The fundamental limitation is the lack of scalability, which this paper will address by exploiting a commercial off the shelf (COTS) technology.

Dual-purpose star trackers offer a unique opportunity for LEO-LEO surveillance. Star trackers are small aperture, wide field of view cameras used for attitude determination. The star tracker captures images of stars and compares the star field to a catalog to determine orientation. They occasionally image and filter other point source objects with

similar brightness to stars, which may be other RSO. A dual-purpose star tracker is one that provides both attitude information and detects, tracks, characterizes and identifies other RSO [8]. Considering the thousands of star trackers already in orbit, a virtual surveillance network for LEO-LEO can be established using existing space infrastructure.

The goal of this paper is to study virtual constellations of dual-purpose star trackers for LEO-LEO SDA and establish the capabilities, requirements and constraints. Section 2 outlines the approach adopted, along with related research in the field of passive optical SDA and mechanics of RSO observation. Section 3 describes the simulation environment and scenarios considered. Section 4 discusses simulation results and their contributions to SDA.

2. APPROACH AND RELATED WORK

2.1 Small Aperture, Wide Field of View

There are two primary modes of passive image capture for wide field of view photography. Stare mode is defined as when an instrument has no active pointing. Sidereal stare mode is a special case of stare mode for ground-based astrophotography where the star field is being tracked, and appears still. Track rate mode is defined by when a target is actively being tracked, with varying amounts of pointing control. This research will primarily consider stare mode, and will be further detailed below.

Stare mode imagery for RSO detection and characterization has been studied extensively in the past. One of the largest publicly available data for this study are from the fast auroral imager (FAI) on-board the CASSIOPE spacecraft [9] [10]. An early feasibility on RSO detection from FAI images concluded that 1 m and 10 m sized objects are detectable at 1,000 km and 10,000 km, respectively [11]. Conclusions also suggested that dedicated commercial star trackers can detect more than 1,200 RSOs daily [12]. This data was used to develop, calibrate and verify a space-based optical image simulator (SBOIS) [13] for the purpose of duplicating FAI images. Continuing research in this field have also led to the development of an image processing framework, like RSOnet, designed to automate image processing and data extraction [8]. Part of the data extracted attempts to duplicate star tracker-based attitude estimation, and has added functionality for RSO detection, tracking, characterization and classification using convolutional neural networks (CNN).

RSONAR is a sub-orbital mission designed for field testing the small aperture, wide field of view method of observation. This mission is part of the Canadian space agency's (CSA) Flights and Fieldwork for the Advancement of Space Technologies (FAST) grant, and was designed to study space-based space surveillance mission concepts. The mission launched in August 2022 with a 2U CubeSat payload mounted on a stratospheric balloon gondola up to an altitude of 37 km. The primary payload was a PCO Panda 4.2 with a 29.7° field of view camera with an aperture of 57 mm, and a Pynq Z1 Xilinx board equipped with a field programmable gate array (FPGA). Preliminary results confirm more than 500 RSO detections during 7 hours of night time imaging. In the coming months, this data will be further analyzed and improvements will be suggested as part of the next mission. This mission and research only considers stare mode, as the design is intended to be non-invasive to existing satellite and gondola scheduling and pointing.

2.2 Resident Space Object Detection

The probability of RSO detection using a satellite mounted camera is dependent on several factors. Most RSO do not emit light of their own, and hence RSO detection relies on the viewing geometry of the Sun, RSO and the observer. Brightness of the Moon and Earth reflecting off the RSO are not considered in this research due to negligible effects. The definition of an RSO detection can be broken down further. The first step is to determine the visual magnitude of the RSO, then compute how much of the RSO-reflected light is captured by the camera and then to use an image processing algorithm to process the detection.

2.2.1 Visual Magnitude of RSO

The visual magnitude, or brightness at a distance, of an RSO depends on the size, shape, albedo, distance, and solar phase angle. Equation 1 below describes this relationship. Each RSO is modeled as a Lambertian sphere [14] [15], having a diffusive reflective property.

$$F_{diff} = \frac{2\,a\,r_{RSO}^2(sin(\phi) + (\pi - \phi)cos(\phi))}{3\pi D^2} \tag{1}$$

In equation 1, a is the albedo, r_{RSO} is the radius of the RSO, ϕ is the solar phase angle and D is the distance between the observer and the RSO. This equation determines the fraction of incident solar flux reflected by the RSO as measured from a distance D. Equation 2 below defines how the incident solar flux of the RSO is used to calculate the visual magnitude of the RSO, m_{RSO}, from an observer.

$$m_{RSO} = -26.74 - 2.5\,log(F_{diff}) \tag{2}$$

where -26.74 is the visual magnitude of the Sun.

2.2.2 Signal to Noise Ratio

The amount of light reflected off the RSO captured by a camera at a defined distance depends as follows. Research conducted in previous efforts [16] [17] [18] describes the relationship between aperture size, quantum efficiency of the sensor, and exposure time and their effect on the signal to noise ratio (SNR). First, the brightness of the RSO, B_{RSO}, is computed as per Equation 3 below.

$$B_{RSO} = I_{RSO}\,A\,e\,Q_{eff} \tag{3}$$

where I_{RSO} is the irradiance of the RSO, A is the surface area of the aperture, e is exposure time and Q_{eff} is the quantum efficiency of the image sensor. The FAI specifications are used for exposure time and quantum efficiency. Next, the SNR is calculated by estimating brightness of the background noise B_{noise} and the image sensor's read noise B_{rd}. These values are calibrated according to the FAI, and will be further described in section 2.3. Equation 4 below illustrates how SNR is computed [18].

$$SNR = \frac{B_{RSO}}{\sqrt{B_{noise} + B_{rd}^2}} \tag{4}$$

For computing the irradiance of the RSO in Equation 3, Equation 5 below is used [17].

$$I_{RSO} = 5.6 \times 10^{10 - 0.4\,m_{RSO}} \tag{5}$$

where m_{RSO} is magnitude of the RSO from Equation 3.2. Using Equations 1 through 5, the SNR of all potential RSO-observer interactions is computed.

2.3 Space-based Space Surveillance using Star Trackers

A large constellation-based approach to space surveillance has several advantages such as geographical distribution, potential for multi-site observations, and redundancy in surveillance infrastructure. Similar constellation-based simulations have previously been studied with up to 24 satellites [19] and show promising results with regards to RSO detection and catalog maintenance. Some mission proposals suggest a dedicated satellite constellation with instrument aperture sizes ranging between 13.7 and 30 cm in diameter. A key conclusion from previous works identify that the dawn-dusk sun synchronous orbit is ideal for multiplicity of RSO detections. This will be described further in Section 3. This research recognizes that launching a large number of satellites for the sole purpose of space surveillance may exacerbate the space debris issue, and considers only hosted-payload solutions.

This research proposes the dual purpose star tracker as an instrument for space surveillance, leveraging existing COTS technology and infrastructure, launch integration and mission support operations and existing data collection capacity. To mimic COTS star tracker specifications, apertures of size 2, 5, 10 and 15 cm will be considered. The field of view will be fixed at 30°, and the exposure time will be limited to 0.1 s. These specifications will allow the star tracker to perform within existing constraints, while provided sufficient functionality to survey for RSO in vicinity. The key trade-off to consider is the instantaneous field of view (IFOV) which is defined by the angular size of one pixel. With an image resolution of 2048 pixels square, our hypothetical instrument has an IFOV of 52.7 arcseconds. Interpolating from previous efforts [8], this represents a Star centroiding accuracy of 10 arcseconds, which is considered suitable for attitude estimation.

3. VIRTUAL CONSTELLATION ANALYSIS SIMULATOR

3.1 Objective and Scope of Simulation

For the objectives of this research, a simulation environment that replicates potential RSO-observer interactions at scale is required. Orbital propagation tools with the capacity to accurately simulate orbits already exist. Systems tool kit (STK) and SBOIS [20] are two such previous efforts. STK and SBOIS take effort to accurately propagate orbits with ephemeris data, which describe the position and velocity of an RSO and also the attitude or pointing direction. This requires obtaining ephemeris data of existing and future satellites expected in this decade. The virtual constellation analysis simulator (ViCAS) presented in this research is a statistical and numerical simulator designed to simplify propagation and large scale modeling of RSO-observer interactions. ViCAS focuses on the spatial densities of RSO in an attempt to discover which orbits, camera mounting configurations and specifications are best suited for observers. The simulator has capacity to propagate the 26,000 RSO currently tracked by SSN, but also model into the future with more than 50,000 RSO. The virtual constellation network configuration, size, and orbits have been defined based on existing, planned and recommended future constellations. ViCAS is also a Python-based open sourced simulator. RSO orbit simulation is simplified using quaternion rotation functions, by defining the key reference frame responsible for optimizing detections [21] [22] [23]. Figure 1 below illustrates the Geocentric Celestial Reference Frame (GCRF) adopted for the simulator. The Sun lies on the ecliptic plane, where as the spin axis of the Earth, which is perpendicular to the equatorial plane, is tilted by 23.4°. The terminator marks the line dividing the Earth into two equal sized hemispheres, one with sunlight and the other in shadow. The terminator is actually a gradient between sunlight and darkness due to atmospheric scattering, however this definition will not be considered in this research due to it's negligible effects on RSO detection from space. Figure 1 below provides a visualization.

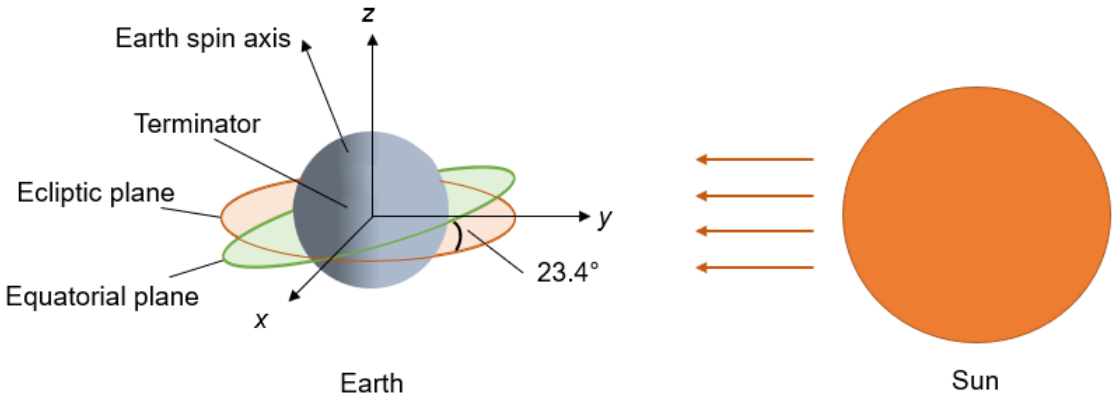

Fig. 1: Visualizing key reference frames for optical RSO detection

Various orbits can be defined using quaternion rotations about the reference frame. Table 1 below identifies the key orbit classes utilized in ViCAS.

Table 1: RSO Orbit Classes defined in ViCAS

Orbit Class	Defined Inclination	Axis of Rotation	Axis of Phase
Dawn-Dusk	98°	Y	N/A
Sun Synchronous	98°	X and Y	Z
Polar	near 90°	X and Y	Z
Low Inclination	80° or below	Earth spin axis	Z

Sun-synchronous orbits closely lead, lag or match the terminator over the course of the year. A dawn-dusk orbit is a special case of a sun-synchronous orbit where the orbit matches the terminator, ensuring the Sun is always on the same side of the satellite. The 98° inclination is further refined depending on mission requirements to revisit the same position on the Earth's surface at the same time every day. In ViCAS, the Sun-synchronous class orbits rotate about the X and or Y axis depending on the phase shift applied along the Z axis. Polar orbit ground-tracks pass closely by the Earth's poles, and are popular for high latitude applications. Low inclination orbits, generally prograde but may also be retrograde, service the middle latitudes where a majority of the Earth's population resides. This technique allows for nearly all LEO classes to be simulated using ViCAS. Visual examples of each orbit are shown below in Figure 2.

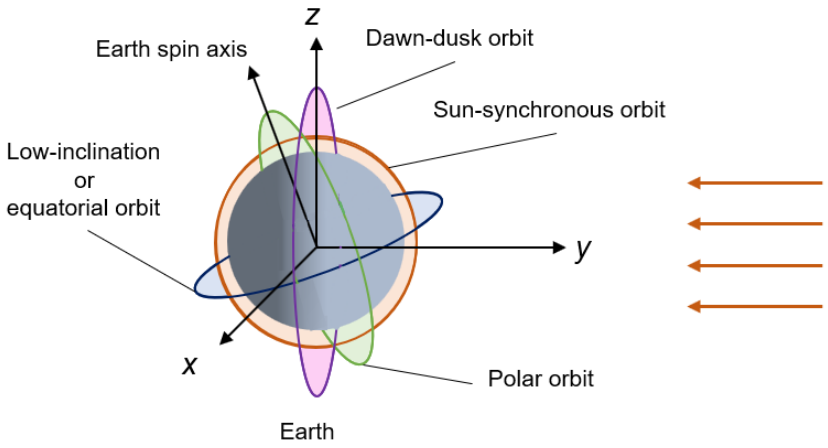

Fig. 2: Visualizing examples of the orbital classes in ViCAS

ViCAS is designed to take as input an RSO base load, which defines the Earth RSO population. A second input defines the virtual constellation configuration. A time step function propagates orbits and observer pointing direction as per a defined step size. All observers follow an Earth-pointing scheme, where the nadir vector points at the center of the Earth. Figure 3 below illustrates this point.

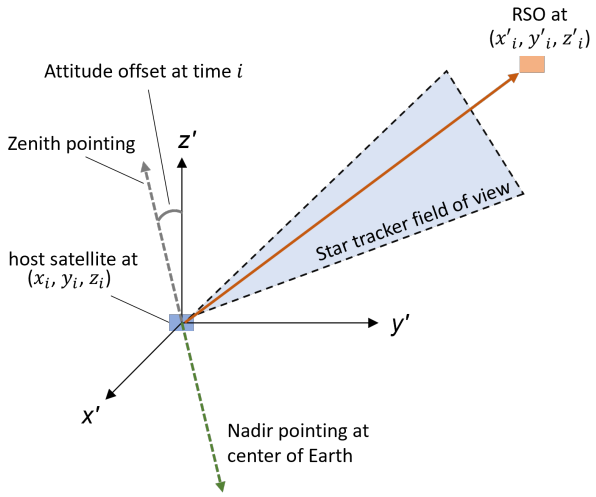

Fig. 3: Visualizing host satellite attitude and relative RSO positioning

At each time step, all potential RSO detections are computed using Equations 1 to 5 and the necessary data is recorded. Processed over several time steps, a simulation scenario is generated.

3.2 Earth $E_\emptyset$

Earth $E_\emptyset$ is defined as the current base load, and is generated using current RSO demographic characterization. The characterization of RSO for ViCAS is defined using size, inclination and altitude. The size distribution is divided into 3 bins, centered at 10 cm, 1 m and 10 m. The total RSO pool for each size bin is a scalable form of the RSO size distribution function [19]. The orbital inclination and altitude distribution of the current base load [24] is also a scalable input.

RSO orbit inclination, altitude and size are not enough characteristics to define unique orbits in ViCAS. The position of an RSO along it's orbital arc is determined by a random rotation along its axis of rotation. The phase of the orbit is determined by an even spacing of all RSO at the same inclination and altitude. These techniques allow for easy constellation mapping on to ViCAS reference frame. The scalable functions for size, inclination and altitudinal distribution of RSO allow for easy scaling operations to study future Earth scenarios. Following this format, Earth $E_\emptyset$ is the standard base load applied to all Earth scenarios considered in this research. Earth E_n defines an Earth n years into the future.

3.3 Simulation Scenarios

Future RSO demographic modeling of RSO has proven to be highly unpredictable, as the true value depends on economics, launch cadence, launch capacity, ride sharing and other factors. Instead, this research will consider a few scenarios for a comparison study. The first scenario considered is the Starlink constellation by Space Exploration Technologies Corporation or SpaceX [25]. There are nearly 2000 Starlink satellites already in orbit and that number is expected to double in the next 2 years. Following this trend, the Starlink scenarios are considered at 0, 2, 4, 6 years into the future defined as $E_{Starlink}$. The second scenario considered is one proposed by this research as potentially the most efficient scenario. A group of dawn-dusk sun-synchronous orbit satellites with a projected count of 100, 500, 1000 and 2000 defined as E_{SSO}. The final scenario considered is a random subset of the overall base load as the base load increases naturally over time. At random, 5% of the overall active satellite base load is converted into an virtual constellation, orbit irrelevant. This scenario is defined as E_{Base}. A summary of the scenarios considered in this research is presented in Table 2 below.

Table 2: Virtual Constellations and RSO population scenarios for comparison

	$E_\emptyset$	E_2	E_4	E_6
$E_{Starlink}$	2,000	4,000	7,000	10,000
Dawn-Dusk or E_{SSO}	100	500	1,000	2,000
5% of base load or E_{Base}	1,300	1500	2,000	2,500
Projected RSO base load	26,000	30,000	40,000	50,000

Each constellation scenario consists of various kinds of orbits distributed depending on the mission objectives. For example, $E_{Starlink}$ [26] is a LEO communication satellite constellation which relies on low-inclination, low altitude orbital shells to provide wide network coverage. The E_{SSO} constellation is a virtual grouping of all the dawn-dusk orbit satellites at varying altitudes. The E_{Base} constellation is the control scenario. A summary of each constellation's breakdown is provided in Table 3 below.

Table 3: Constellation scenarios and parameters that define them

Constellation Scenario	Inclination (°)	Altitude (km)	Share of Total
$E_{Starlink}$	50±5	550	66.7%
	70±5	550	11.1%
	90±5	550	11.1%
	98	550	11.1%
E_{SSO}	98 (dd)	400	20%
	98 (dd)	800	20%
	98 (dd)	1000	20%
	98 (dd)	1400	20%
	98 (dd)	1800	20%

(dd) refers to the dawn-dusk classification of the sun-synchronous orbit

3.4 Simulation Context

Some important ViCAS assumptions are listed below:

- ViCAS identifies an RSO detection valid above an SNR of 3. Although this detection sensitivity is difficult to achieve on a reliable basis, ViCAS demonstrates the potential of the instrument.
- The exposure time for all star tracker images are fixed at 0.1 seconds. A longer exposure time may skew the results in favour of more detections than is otherwise possible with a stare-only camera.
- Every time step is defined at 10 seconds, and every scenario is 24 hours long. This means that the set duty cycle of the star tracker is 1%. At every time step, the detection statistics are computed and recorded for post processing.
- All RSO detections are range limited to 300 km. This is to minimize simulation time. Based on this assumption, for larger aperture cameras, the detection estimates are considered conservative.

4. SIMULATION RESULTS

4.1 Number of Detections

The light collecting area, proportional to the square of the aperture size, has a significant impact on the RSO detections possible. Figure 4 below compares the number of RSO detections, in thousands, over the course of 24 hours for

$E_{Starlink}$ with varying aperture sizes. Depending on the aperture size, the results suggest that Starlink may currently be able to detect between 6,000 to 158,000 RSO daily, which translates to 3 - 79 RSO per satellite per day. A majority of these detections are from the sun-synchronous and polar orbiting satellites of the constellation. Figure 5 below illustrates how with just 100 satellites as part of E_{SSO}, the potential detection counts range between 1,000 and 43,000, equivalent to 10 to 430 detections per satellite. Figure 6 represents the random adoption of active satellites, and at current capacity, the detection potential ranges from 7,000 to 44,000, or 5 - 34 per satellite.

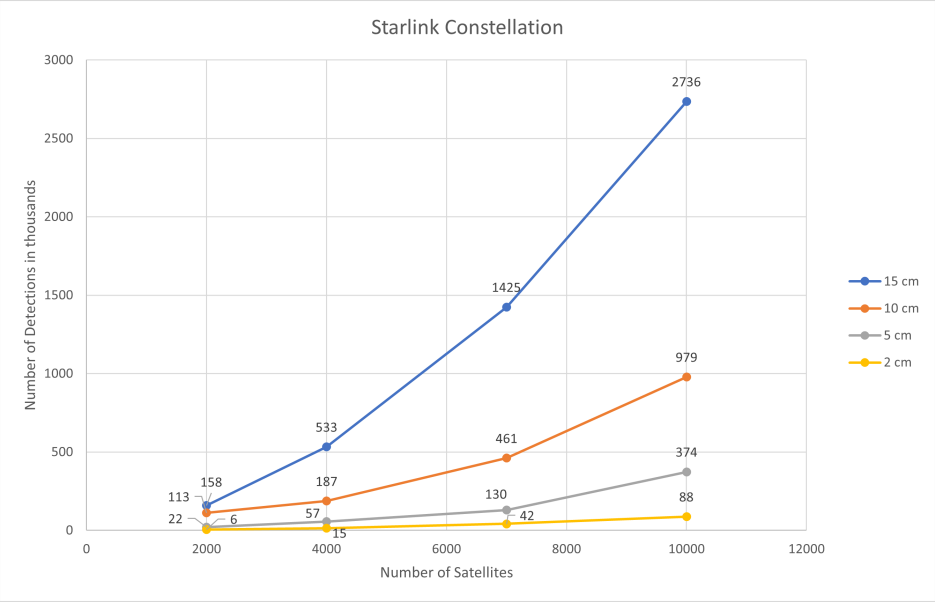

Fig. 4: Number of potential RSO Detections from $E_{Starlink}$ daily

Fig. 5: Number of potential RSO Detections from E_{SSO} daily

For each scenario, the direction of mounting has varying impacts on the number of RSO detections. For $E_{Starlink}$, 96% of detections are evenly split between ram, anti-ram, port and starboard, with the remaining 4% in the zenith direction. For E_{SSO}, on average the port direction is ideal with over 72% of detections with the remaining split between ram and

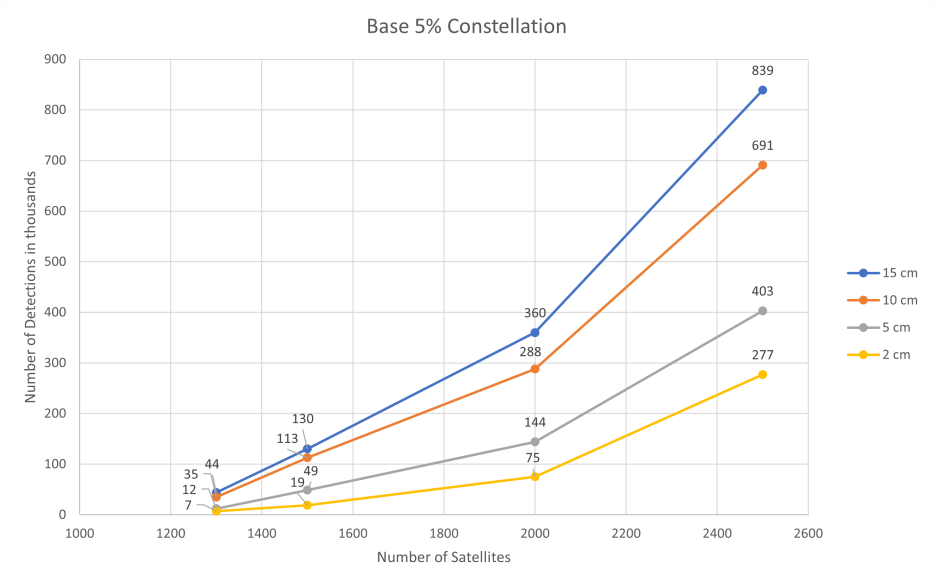

Fig. 6: Number of potential RSO Detections from E_{Base} daily

anti-ram, with leftovers for zenith and none for starboard. This conclusion is expected for the sun-synchronous orbit, as port direction is the anti-sun direction and starboard faces the sun. For E_{Base}, port and starboard split 60% of the detections while the remaining 40% is split between ram and anti-ram. Compared to previous efforts [11], ViCAS supports the directional mounting benefits and drawbacks.

Figure 7 compares the scenarios with the number of detections as a function of the number of satellites. Despite E_{SSO} being by far the most efficient of the scenarios considered, $E_{Starlink}$ remains the most practical and easy to scale with. This is especially due to Starlink design consistency across thousands of satellites.

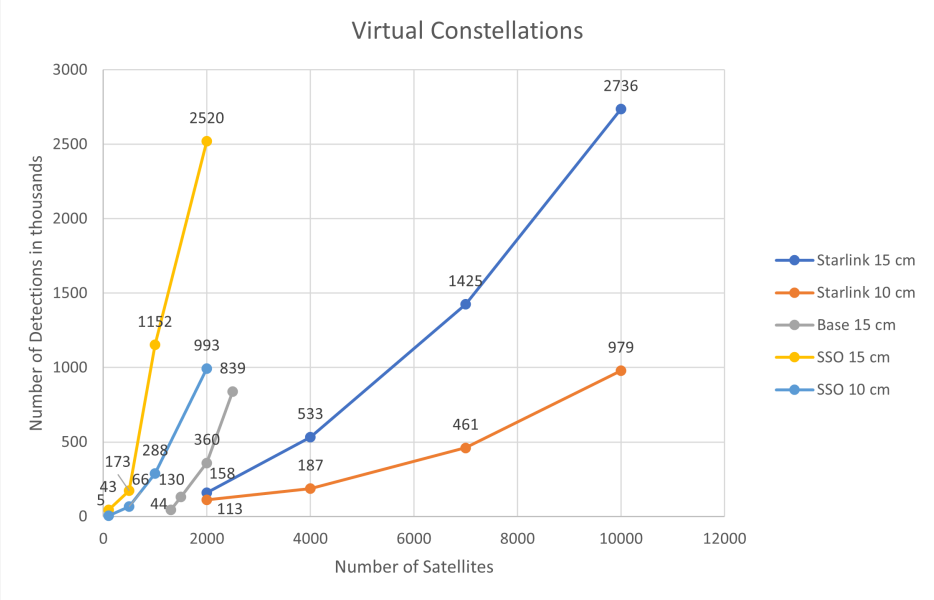

Fig. 7: Number of daily potential RSO Detections for $E_{Starlink}$, E_{SSO} and E_{Base}

One of the most important advantages of constellation-based approach to SDA is the likelihood of multi-site detections,

where one RSO is being simultaneously observed by 2 or more observers. Multi-site observations can counter the low capability of an individual star tracker, allowing orbit determination algorithms to converge faster and more accurately on a solution. For the scenarios considered in Figure 8, the multi-site detections are only for the given constellation, and do not take into account any other ground or space-based instrument. This also implies that large volumes of non-multi-site detections can actually be multi-site when accounting for other SSN instruments.

Fig. 8: Number of daily potential Multi-site Detections

4.2 Detection Characterization

In addition to the number of potential detections, the duration of detection is also important for SDA. On average for E_{Base} over 10 simulation cycles, an RSO remains consistently detected for 142 seconds, with a σ of 18 seconds. For $E_{Starlink}$, the average duration of detection is 130 seconds, with a σ of 9 seconds. Smaller aperture sizes do not have a significant impact on the duration, as the missed detections are wholly absent from the detection pool. For E_{SSO}, the average duration of detection is 167 seconds, with a σ of 28 seconds. Due to near-ideal port-facing solar phase angles for E_{SSO}, the average is considerably higher. In the scenarios considered, on average over 2 minutes of continuous observation is expected. The RSO, however, is only out of view temporarily as it is likely to be detected by another observer with a shorter revisit time.

Revisit times are a decided advantage of a virtual constellation at scale, ensuring a satellite remains out of view for a minimal period. This is of key interest to national security needs. ViCAS does not currently calculate revisit times as part of its simulation, and is planned as a future upgrade. However, the percentage of time each RSO is detected by at least one observer is recorded. The averaged solution is shown in Table 4, separated by scenario, year of simulation and aperture sizes. In some cases, certain RSO are detectable over 21% of their orbital trajectory by various observers.

Table 4: Average detection coverage over all RSO simulated

	5 cm	10 cm	15 cm
$E_{\emptyset Starlink}$	0.1%	0.1%	0.4%
$E_{6Starlink}$	0.5%	1.3%	3.9%
E_{6SSO}	0.1%	0.5%	3.5%
E_{6Base}	0.2%	0.6%	2.4%

Additionally, faster revisit times also benefits satellite re-entry analysis, especially in cases where the YarkovskyO'Keefe-Radzievskii-Paddack (YORP) effect [27] can vary the debris landing site significantly, as was the case for the Chinese Long March 5B upper stage rocket. In context of conjunctions and debris avoidance, NASA begins with conjunction data messages (CDM) 7 days prior to a possible debris avoidance maneuver for the international space station (ISS) [28]. Faster revisit times also reduce the amount of uncertainty in projecting if a piece of space debris is of risk to an asset, with potential to generate more accurate CDM, and provide suitable orbits to minimize future debris avoidance maneuvers.

Another key metric for RSO characterization is the ability view the object from varying attitudes. From a ground-based observer, it is likely that the same facet of a satellite may be visible at every pass. For LEO-LEO observations, the facets are randomized to some extent. The advantage of accumulating a holistic views of the RSO catalog over time provides better information on expected shape estimated for improved propagation results.

5. DISCUSSION

In context of the results presented above, there are significant advantages to a distributed method of data collection for SDA. Each node of the virtual network is significantly cheaper to build, operate and replace. A significant part of the cost advantage is due to the hosted payload concept on soon to launch space infrastructure. Another key factor is automation, allowing for ease of scaling due to commonalities and standardization in hardware and communications. Preliminary resource requirement estimates suggest power, thermal and data rate requirements fit CubeSat payload budgets. Estimates of power consumption under 5 Watts, and data rate less than 100 kbps are feasible for a dual purpose star trackers with a high compression ratio [8]. Resource consumption efficiency and image capture optimization can be achieved with improved payload duty cycling based on opportunistic scheduling.

Some of the shortcomings of the virtual constellations concept include scaling issues due to technology adoption. Scalability is key to the independent success of the concept, however even limited scaling can obtain partial success when observations are made in blind spots of other instruments, or as part of a multi-site observation. Part of the adoption challenge pertains to data downlink rate and latency required for real-time SDA. In addition, high-grade timing and position information of the observer are required for accurate RSO orbit characterization.

Despite the promising simulation results and uncertainties of the concept, real data at a large scale is required to verify these conclusions in a practical sense. RSONAR is one such concept demonstration mission which has shown the benefits of small aperture, wide field of view photometry for RSO detection. As indicated earlier, preliminary results suggest that over 500 unique RSO sequences have been captured and further processing of the data will help improve simulation models such as SBOIS and ViCAS.

6. CONCLUSIONS

In conclusion, this research demonstrates that a virtual constellation of dual-purpose star trackers can offer a unique and valuable contribution to the data collection capacity of any SDA system. If the scalability can be achieved, a majority of the LEO RSO population can be kept under near constant surveillance. Even in limited capacity, the network recommended can offer key insights in existing SDA blind spots, with the potential to observe unpredictable events in LEO. The instrument design proposed is geographically distributable, low-cost and scalable, and has the potential to fill existing SDA gaps. There are still several uncertainties pertaining to the quality of detections, and how well they can be used for RSO orbit determination, light curve analysis, identification, characterization and catalog maintenance.

As part of future work, this research recommends algorithm development for how to improve performance and characterization on small aperture, wide field of view RSO imagery. In addition, active tracking can be pursued with algorithms to optimize for viewing direction. Other research in scope of light curve analysis, multi-site analysis and RSO shape and attitude characterization would be of key interest. Pursuing a common star field image processing framework [8], database creation for automation using artificial intelligence algorithms should also be pursued.

REFERENCES

[1] Oltrogge D. The "we" approach to space traffic management. *15th International Conference on Space Operations, 2018*, (June):1–21, 2018.

[2] Jah M. Space surveillance, tracking, and information fusion for space domain awareness. pages 1–18, 2016.

[3] April J. Nanosat employment : a theoretical CONOPS for space object identification NAVAL POSTGRADUATE. 2014.

[4] Stokes G. H., Curt V. B., Sridharan R., and Sharma J. The space-based visible program. *Space 2000 Conference and Exposition*, 11(2):205–238, 2000.

[5] Gaposchkin E. M., Curt V. B., and Sharma J. Space-based space surveillance with the Space-Based Visible. *Journal of Guidance, Control, and Dynamics*, 23(1):148–152, 2000.

[6] Maskell P. Sapphire: Canada's Answer to Space-Based Surveillance of Orbital Objects. *Advanced Maui Optical And Space Surveillance Technologies Conference*, 2008.

[7] Scott R. and Thorsteinson S. Key Findings from the NEOSSat Space-Based SSA Microsatellite Mission. *Advanced Maui Optical and Space Surveillance Technologies Conference*, (October), 2018.

[8] Dave S., Clark R., and Lee R. S. K. Rsonet: An image-processing framework for a dual-purpose star tracker as an opportunistic space surveillance sensor. *Sensors*, 22(15), 2022.

[9] Cogger L., Howarth A., Yau A., White A., Enno G., Trondsen T., Asquin D., Gordon B., Marchand P., Ng D., Burley G., Lessard M., and Sadler B. Fast Auroral Imager (FAI) for the e-POP Mission. *Space Science Reviews*, 189(1-4):15–25, 2015.

[10] Yau A. W. and James H. G. CASSIOPE Enhanced Polar Outflow Probe (e-POP) Mission Overview. *Space Science Reviews*, 189(1-4):3–14, 2015.

[11] S. Clemens. On-orbit resident space object (rso) detection using commercial grade star trackers. *Masters of Science Thesis*, 2019.

[12] Clemens S., Lee R. S. K., and Harrison P. Feasibility of Using Commercial Star Trackers for On-Orbit Resident Space Object Detection Warren Soh. *Advanced Maui Optical And Space Surveillance Technologies Conference*, 2018.

[13] Clark R., Fu Y., Dave S., and Lee R. S. K. Using Parallel Processing. 2021.

[14] Cognion R. L. Observations and Modeling of GEO Satellites at Large Phase Angles. *Advanced Maui Optical and Space Surveillance Technologies*, 2013.

[15] Krag W. E. Visible magnitude of typical satellites in synchronous orbits. 1974.

[16] Hejduk M. and Lambert JV. Satellite Detectability Modeling for Optical Sensors. *AMOS Technical Conference*, pages 101–110, 2004.

[17] Vallado D. *Fundamentals of Aerodynamics and Applications*. 2007.

[18] Howell S. Handbook of CCD Astronomy. *Cambridge University Press*, 2006.

[19] Du J., Chen J., Li B., and Sang J. Tentative design of SBSS constellations for LEO debris catalog maintenance. *Acta Astronautica*, 155(June):379–388, 2019.

[20] Clark R., Dave S., Wawrow J., and Lee R. S. K. Performance of Parameterization Algorithms for Resident Space Object (RSO) Attitude Estimates. *Advanced Maui Optical And Space Surveillance Technologies Conference*, 2020.

[21] Svehla D. Earth orientation quaternion and modeling the satellite orbit using quaternions. *36th Committee on Space Research Scientific Assembly*, page 3034, 2006.

[22] Svehla D. *Geometrical Theory of Satellite Orbits and Gravity Field*. 2018.

[23] Libraro P., Kasdin N. J., Choueiri E. Y., and Dutta A. Quaternion-based coordinates for nonsingular modeling of high-inclination orbital transfer. *Journal of Guidance, Control, and Dynamics*, 37(5):1638–1644, 2014.

[24] Tadini P., Tancredi U., Grassi M., Anselmo L., Pardini C., Branz F., Francesconi A., Maggi F., Lavagna M., De Luca L. T., Viola N., Chiesa S., Trushlyakov V., and Shimada T. Active debris removal space mission concepts based on hybrid propulsion. *Proceedings of the International Astronautical Congress, IAC*, 3(August 2015):2319–2328, 2013.

[25] SpaceX Designing and Building Safe , Reliable and Demisable Satellites Extremely Low Orbit Insertion Operating Below 600 km. 2022.

[26] McDowell J. Jonathan's Space Report — Space Statistics. 2019.

[27] Benson C. J., Naudet C. J., Scheeres D. J., Jao J. S., Snedeker L. G., Ryan W. H., E. V. Ryan, Silva M. A.,

Lagrange J. K., Bryant S. H., Tsao P. C., Lee D. K., Yildiz U., and Nguyen H. D. Radar and Optical Study of Defunct Geosynchronous Satellites. *Journal of the Astronautical Sciences*, 68(3):728–749, 2021.

[28] Newman L. K., Mashiku A. K., Hejduk M. D., Johnson M. R., and Rosa J. D. Nasa conjunction assessment risk analysis updated requirements architecture. *Advances in the Astronautical Sciences*, 171:3485–3504, 2020.